Fragility of Reinforced Concrete Framed Structures to Flow-type Landslides

Fulvio Parisi
Assistant Professor, Dept. of Structures for Engineering and Architecture, University of Naples Federico II, Naples, Italy

Giuseppe Sabella
Research Fellow, Dept. of Structures for Engineering and Architecture, University of Naples Federico II, Naples, Italy

Carmine Galasso
Lecturer, Dept. of Civil Environmental & Geomatic Engineering and Institute for Risk and Disaster Reduction, University College London, UK

ABSTRACT: Flow-type landslides are typically triggered by heavy rainfalls and may cause large losses. Landslide risk may be rationally evaluated and mitigated with probabilistic approaches. In this paper, physical vulnerability of reinforced concrete buildings to landslides is assessed. Fragility analysis was carried out by assuming flow velocity as intensity measure, several damage states, and different mechanical models for beams, columns and masonry infill walls. Uncertainties in landslide impact loading, material properties, members geometry, and capacity models were taken into account. Both earthquake-resistant and gravity-load designed buildings were assessed as being representative of two low-rise building subclasses. Analysis results show that landslide fragility significantly depends on the presence and type of infill walls, which influence both out-of-plane and in-plane failure modes as well as yielding and failure of plastic hinges in columns.

1. INTRODUCTION

Every year landslides occur all over the world as a result of several triggering events such as rainfalls and earthquakes, causing fatalities and heavy damage to buildings and infrastructure systems. The EM-DAT International Disaster Database (Sapir and Misson, 1992) highlights that 671 landslides have occurred between 1900 and 2014, affecting 13,700 million of people and causing more than 65,000 casualties and an economic loss greater than 8.7 billion USD. Recent studies have also shown that the amount of landslides and victims is an order of magnitude greater than above (Petley, 2012). Therefore, landslide risk governance is a key challenge for modern society and may be rationally dealt with quantitative risk analysis (Corominas et al., 2013). Such an approach provides the probability of exceeding a prescribed loss level in a given spatio-temporal scale, considering uncertainty in hazard, exposure and vulnerability of elements at risk, e.g. houses, lifelines and people. Setting up a probabilistic framework for landslide risk analysis allows scientists and decision makers to overcome limited and/or purely qualitative information provided by landslide susceptibility and hazard maps, which are the most common tools so far.

Several types of landslide vulnerability may be assessed, that is physical, socio-economic and environmental vulnerabilities. As far as physical vulnerability of elements at risk is concerned, a significant knowledge gap affects the assessment of the landslide vulnerability of buildings. Physical vulnerability may be evaluated through expert opinion (judgmental methods), damage data from past events (empirical methods), or mechanical

models (analytical methods). Moreover, depending on the territorial scale adopted for landslide risk analysis, vulnerability assessment may focus on either individual buildings or building classes.

This paper investigates the vulnerability of reinforced concrete (RC) framed building structures to flow-type slides, which are rapid landslides with high proportion of water to solid material. This study is motivated by the fact that RC buildings are a large fraction of the worldwide built heritage, providing a major contribution to landslide risk in many regions, particularly in the Euro-Mediterranean area. Also, flow-type slides are among the most destructive landslides and are typically triggered by heavy rainfalls or rapid snowmelt. Herein, landslide vulnerability is assessed by means of fragility analysis, which is a well-established tool in earthquake engineering (Porter et al., 2007) and has been recently used for vulnerability assessment to landslides (Fotopoulou and Pitilakis, 2013) and other natural hazards, e.g. flood (Pregnolato et al., 2015). The analysis output consists of fragility curves associated with different damage states for landslide loss assessment.

2. METHODOLOGY

Fragility analysis is an effective procedure to assess the probability of exceeding a certain damage state/level as a function of a scalar or vector-valued intensity measure (IM). Mavrouli et al. (2014) evaluated the flow-type landslide fragility of single-bay, single-story RC frames with low, medium and high ductility. In this study, two-story, double-bay, 2D RC frames are considered as subsystems taken out from 3D framed structures. The building is supposed to have a shallow stiff foundation, so that a fixed base is assigned to columns of frame models. Several variants of 2D frames were set up to account for structural characteristics and contribution from infill walls. Therefore, two building subclasses were assessed:

- Low-rise RC buildings designed only to gravity loads without any seismic detailing (Masi and Vona, 2012);
- Low-rise RC buildings designed for earthquake resistance according to the high ductility class of Eurocode 8 (EC8) – Part 1 (CEN, 2004).

According to the typical taxonomy adopted in seismic risk assessment, the former may be defined as pre-code subclass, the latter is a special-code subclass. As flow-type landslides such as debris and mud flows are considered (Figure 1), the flow velocity was assumed as IM, being it significantly correlated with damage (e.g. Mavrouli et al., 2014). Several damage states were assumed and then the landslide vulnerability of case-study RC buildings was assessed for each of them, assuming different engineering demand parameters (EDPs) to quantify landslide demand on the structure. For each building subclass, fragility analysis consisted of the following steps: (i) a Monte Carlo simulation to randomly generate realizations of both load conditions and structural systems within the subclass, based on probability distributions for material properties, geometrical parameters and structural capacity model to account for uncertainty in structural capacity; (ii) nonlinear analysis of the structure at different IM levels; (iii) fragility estimation by convolution of demand and capacity for each damage state; and (iv) fitting of lognormal fragility functions (e.g. Porter et al., 2007).

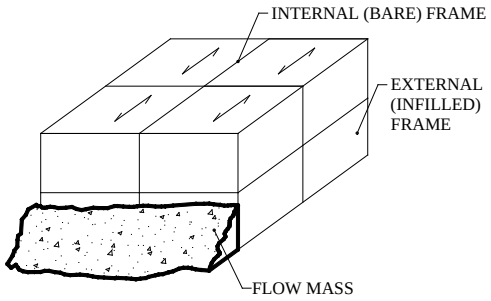

Figure 1: RC framed building impacted by flow-type landslide.

2.1. Damage states

The landslide impact loading on the RC building may have different effects on both masonry infills and RC structural members. Hence, a set of damage states must be considered and eventually associated with different EDPs. According to damage observed after past flow-type landslides, four damage states may be assumed as follows:

- DS1: out-of-plane collapse of infill walls of the building perimeter;
- DS2: in-plane cracking of infill walls;
- DS3: yielding rotation of a plastic hinge in a column;
- DS4: ultimate rotation of a plastic hinge in a column.

DS1 is significantly different from other damage states as it is associated with external infilled frames that are transversally impacted by the flow. Masonry infill walls may suffer out-of-plane collapse by three-hinge mechanism or shear sliding. Damage states from DS2 to DS4 are associated with in-plane lateral loading of orthogonal RC frames. If an internal 2D frame is considered, infill walls may be lacking so that DS2 may not apply. As a result, in-plane lateral loading may cause the attainment of DS3 and DS4. Otherwise, if an external 2D frame is assessed, masonry infill walls are typically present and may suffer different types of failure under in-plane lateral loads. In that case, DS2 is of interest for vulnerability assessment.

2.2. Modeling of landslide impact load

Flow-type landslides include, among other movements, debris flows and mudflows. A debris flow is a very rapid to extremely rapid movement of a mixture of loose granular soil, rock, organic matter, air and water. A mudflow is a rapid movement of fine-grained soil with a water content of up to 60%. Catastrophic effects on buildings may be induced not only by the high density, depth and velocity of the soil mass, but also by the impact of objects such as vehicles which are dragged by the flow. Based on momentum equation, the dynamic impact pressure of the flow was predicted as follows:

$$p_d(z_s) = \rho g (D - z_s) + \rho v^2 \cos^2\theta \qquad (1)$$

where: ρ = flow density; g = acceleration of gravity; D = flow depth; z_s = depth of generic soil layer from the free surface of the flow; v = flow velocity; and δ = angle of flow direction with respect to the axis perpendicular to the impacted surface. In this study, the authors assume the most demanding load related to a building side impacted by a perpendicular flow (i.e. δ = 0). Objects dragged by the flow are not considered in the fragility analysis. The inclusion of their impact force as conditional or additional IM is currently under investigation. Eq. (1) provides the dynamic impact pressure over a surface element of the building façade. This pressure is assumed to consist of a geostatic component and a kinematic component, which are linearly and uniformly distributed over the flow depth, respectively (Figure 2). It is noted that $D = \xi h_i$ is the height of the surface element impacted by the landslide, where ξ = fraction of interstory height. The lateral load q_d (z_s) per unit height of building façade depends on the effective width b_{eff} of the surface element, as follows:

$$q_d(z_s) = p_d(z_s) b_{eff} \qquad (2)$$

To assess landslide fragility of infill walls, a unit width was considered. To assess landslide fragility of RC frames, the lateral load was applied to external columns of a building side. Two alternative widths were considered, depending on the presence and effectiveness of shear connection between RC columns and adjacent infill walls. Denoting by b the column width and l_w the length of adjacent infill walls, the effective width was assumed as $b_{eff} = b + \beta l_w$ where β was set to 0.5 in case of corner column, i.e. external infilled frame, and 1 in case of intermediate column, i.e. internal bare frame.

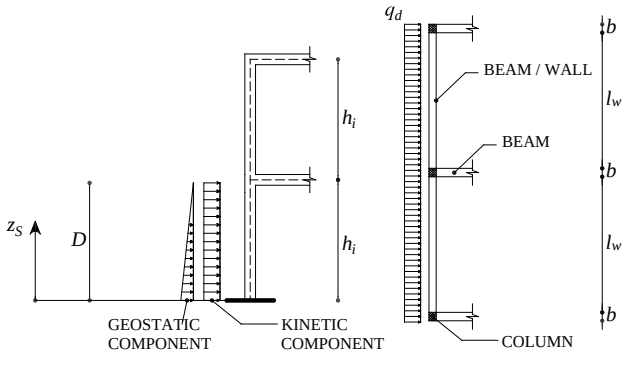

(a) (b)

Figure 2: Impact load on building façade: (a) lateral view; (b) plan view.

When shear sliding strength of the column-wall mortar joint was exceeded, the authors set $b_{eff} = b$. An equivalent uniform lateral pressure p_{eq} was derived from the actual pressure profile $p_d(z_s)$ to assess infill walls under out-of-plane loading. The equivalent pressure was computed through *Mathematica*®, assuming the same external work done by the actual and ideal pressures as the infill wall experiences out-of-plane displacements.

2.3. Capacity models

The authors developed three capacity models: (i) infill wall subjected to out-of-plane loading; (ii) 2D bare frame subjected to in-plane loading; and (iii) 2D masonry infilled frame subjected to in-plane loading. The out-of-plane lateral strength of the infill wall against three-hinge collapse mechanisms was predicted as follows (Abrams et al., 1996):

$$w = \frac{0.7 f_w \lambda}{h_w / t_w} \tag{3}$$

where: f_w = uniaxial compressive strength of masonry; h_w = infill wall height; t_w = infill wall thickness (its solid fraction in case of two-wythe masonry wall with internal cavity); and λ = dimensionless factor related to the compressive stress field. The out-of-plane strength was set to the minimum between w and masonry strength associated with sliding out-of-plane mechanism.

The capacity model used for masonry-infilled RC frames consisted of a frame with diagonal struts able to resist only in compression (Bertoldi et al., 1993; INRC, 2013). The structural model was developed in *OpenSees*® (McKenna et al. 2004). Each strut was modeled as single truss element with rectangular cross section and axial plastic hinge at the midspan section. The thickness t_w and width b_w of the strut section were defined according to Stafford Smith (1966). The axial load capacity of the internal strut was assumed to be

$$N_{wu} = f_{wu} b_w t_w \tag{4}$$

where f_{wu} is the minimum value of four strengths associated with the following failure modes: (i) crushing at the wall center; (ii) crushing at the wall toes; (iii) shear sliding along a mortar bed joint; and (iv) diagonal tension cracking of the wall. The last three failure modes are also considered in case of load-bearing masonry walls (Parisi and Augenti, 2013). The last two failure modes depend on the following: f_{v0} = shear sliding strength of mortar bed joint; and τ_0 = diagonal shear strength of masonry. The authors assumed $f_{v0} = \tau_0$ (IMIT, 2009) and the axial stiffness of the internal strut as

$$k_w = \frac{E_{w\varphi} b_w t_w}{d_w} \tag{5}$$

where $E_{w\varphi}$ = Young's modulus of masonry in the diagonal strut direction. The strut was an elastic-perfectly plastic truss element with ultimate strength N_{wu}, cracking axial displacement u_y and ultimate axial displacement $u_u = \mu_u u_y$ where $\mu_u = 2$.

Either in case of bare or masonry-infilled RC frames, the authors assigned plastic hinges to columns and beams. A multilinear bending moment–chord rotation diagram was assumed in case of EC8-compliant frames (Figure 3a), where: M_y = yielding moment; θ_y = yielding rotation; M_{max} = maximum moment; θ_{Mmax} = rotation at M_{max}; M_u = ultimate moment; and θ_f = ultimate rotation.

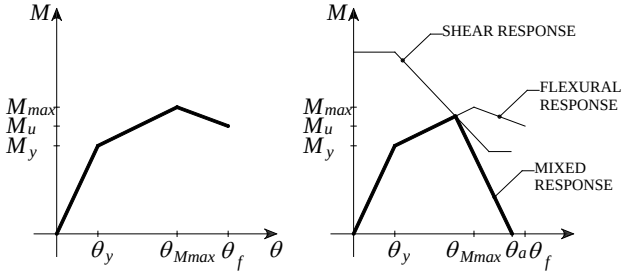

Figure 3: Moment–rotation diagram of plastic hinge in (a) EC8-compliant frame and (b) gravity-load designed frame.

The following rotations were assumed (Fardis, 2007):

$$\theta_y = \frac{\phi_y L_V}{3} + 0.0013\left(1 + 1.5\frac{h}{L_V}\right) + 0.13\phi_y \frac{d_b f_y}{\sqrt{f_c}} \tag{6}$$

$$\theta_{Mmax} = \frac{3}{4}\theta_f \tag{7}$$

$$\theta_f = 0.016 \cdot 0.3^{\nu} \left[\frac{\max(0.01;\omega')}{\max(0.01;\omega)} f_c \right]^{0.225} \cdot \left(\frac{L_V}{h} \right)^{0.35} 25^{\alpha \rho_{sx} \frac{f_{yw}}{f_c}} 1.25^{100\rho_d} \quad (8)$$

where: ϕ_y = yielding curvature; L_V = shear span at member end; h = cross section depth; d_b = mean diameter of tension reinforcement; f_y = steel yield strength; f_c = concrete compressive strength; ν = dimensionless axial load; ω' = mechanical reinforcement ratio of compression reinforcement; ω = mechanical reinforcement ratio of tension reinforcement; α = confinement effectiveness factor; ρ_{sx} = ratio of transverse steel parallel to the loading direction; f_{yw} = stirrup yield strength; and ρ_d = steel ratio of diagonal reinforcement.

In case of gravity-load designed RC frames, the moment–rotation diagram of the plastic hinge was modified to account for shear-flexural interaction (Biskinis et al., 2004; CEN, 2005) and axial load capacity degradation due to shear cracking (Zhu et al., 2007). That diagram was derived as lower envelope of flexural and shear response diagrams (Figure 4b). The shear capacity of slender RC members was defined as

$$V_R = V_N + V_c + V_w \quad (9)$$

where:

$$V_N = \frac{h-x}{2L_V} \min(N; 0.55 A_c f_c) \quad (10)$$

$$V_c = \left[1 - 0.05 \min(5; \mu_{\Delta pl})\right] \cdot 0.16 \max(0.5; 100\rho_{tot}) \cdot \left[1 - 0.16 \min\left(5; \frac{L_V}{h}\right)\right] \sqrt{f_c} A_c \quad (11)$$

$$V_w = \left[1 - 0.05 \min(5; \mu_{\Delta pl})\right] \rho_w f_{yw} b z \quad (12)$$

where: x = compression zone depth; N = compressive axial load; A_c = cross section area; $\mu_{\Delta pl}$ = plastic part of displacement ductility demand; ρ_{tot} = total longitudinal reinforcement ratio; ρ_w = transverse reinforcement ratio; b = cross section width; and z = length of internal lever arm.

In case of shear failure, a linear axial capacity loss may be assumed for plastic hinge up to the following chord rotation:

$$\theta_a = 0.184 \exp(-1.45\mu) \quad (13)$$

where μ = effective friction coefficient over the shear crack surface. Nevertheless, the plastic hinge failing in shear was assumed to have an ultimate rotation associated with the intersection between flexural and shear response diagrams in Figure 4b. That rotation was denoted by θ_v so the ultimate rotation was set to $\theta_u = \min(\theta_f;\theta_v)$ in case of gravity-load designed frames.

3. UNCERTAINTY MODELING

3.1. Demand

Assuming a nominal flow velocity v, the flow density ρ and depth D were considered as uniformly distributed random variables (RVs) of the impact load model. The authors assumed a flow density ranging from $1.4 \cdot 10^3$ to $2.2 \cdot 10^3$ kg/m^3 and a flow depth between $0.5h_i$ and $1.5h_i$. The correlation between flow velocity and depth has not been considered here due to the lack of reliable models for its quantification.

3.2. Capacity

Both gravity-load designed and EC8-compliant frames were supposed to have nominal interstory height h_i = 3 m, nominal span length l = 5 m and deterministic sectional concrete cover of 30 mm. Shear member span was set to half span length. All geometric properties, at both members and cross-sections levels, were assumed to be normally distributed with mean equal to their nominal value and CoV = 4% (Galasso et al, 2014). Probability distributions were meant to characterize uncertainties in structural capacity.

In case of gravity-load designed frames, the authors considered typical materials of residential buildings in Euro-Mediterranean regions before 1971 (Masi and Vona, 2012; Verderame et al., 2001a,b). The classes C10/12 and Aq42 were assumed for concrete and reinforcing steel, respectively. Nominal code values were assigned to strain limits of materials. Weak infill walls

consisting of two hollow clay block masonry wythes with 60% volumetric percentage of holes and internal cavity were considered (Hak et al., 2012). According to INRC (2013), the masonry was assumed to have shear modulus $G_w = 0.3E_{wv}$ and Young's modulus in horizontal direction $E_{wh} = 0.5E_{wv}$. Table 1 outlines the mean and coefficient of variation (CoV) of material properties, which were considered to be lognormally distributed. The same steel type was assumed for longitudinal and transverse reinforcements, that is $f_{yw} = f_y$.

Table 1: Statistics of material properties of gravity-load designed frames.

Variable	*Mean [MPa]*	*CoV [%]*
f_c	*16*	*31*
f_y	*250*	*8*
f_w	*1.5*	*14*
τ_0	*0.31*	*13*
E_{wv}	*1873*	*14*

As far as geometrical properties are concerned, nominal sizes of 300×300 and 300×500 mm^2 were assumed for columns and beams, respectively. Mechanical reinforcement ratios of compression and tension reinforcements, i.e. ω' and ω, were derived from ρ_{tot}. The latter was assumed to be 0.59% in case of columns (Masi and Vona, 2012), and 0.70% in case of beams (Royal Decree, 1939). Instead, ρ_w was set to 0.20% in case of columns (Sezen and Moehle, 2004) and 2.35% in case of beams (Royal Decree, 1939). Dealing with weak infill walls, the unit weight of masonry and wall thickness were assumed to be deterministic properties equal to 7 kN/m^3 and 240 mm, respectively. Finally, the authors considered the uncertainty associated with capacity models of RC members and infill walls. According to Fardis (2007), a Lognormal distribution was assumed for θ_y and θ_f. Mean estimates derived from Eqs. (6) and (8) were multiplied by the bias term, which was respectively set to 1.015 and 0.995. CoV was assumed to be 33.1% and 40.9% for θ_y and θ_f, respectively. The shear capacity provided by Eq. (9) was also assumed to be the mean of a Lognormal distribution with CoV = 25% (Biskinis et al., 2004). The chord rotation θ_a was also considered to be lognormally distributed with mean provided by Eq. (13) and CoV = 35% (Zhu et al., 2007). Uncertainty in the capacity model of infill walls was considered in terms of μ_u. Based on INRC (2013), μ_u was assumed to be a Lognormal parameter with mean equal to 2 and CoV = 25%.

In case of EC8-compliant frames, concrete and steel were respectively assumed to be of class C20/25 and B450C. Table 2 provides statistics of material properties (INRC, 2013; Hak et al., 2012) which were assumed to be Lognormal RVs.

Table 2: Statistics of material properties of EC8-compliant frames.

Variable	*Mean [MPa]*	*CoV [%]*
f_c	*28*	*18*
f_y	*500*	*5*
f_w	*3.5*	*14*
τ_0	*0.11*	*13*
E_{wv}	*3150*	*14*

Infill walls were assumed to be made of a single-wythe hollow clay block masonry with deterministic thickness t_w = 300 mm, volumetric percentage of holes in blocks lower than 45%, and dry vertical joints. A deterministic unit weight of 11 kN/m^3 was assumed for masonry. Columns and beams were assumed to have nominal size of 300×600 and 300×500 mm^2, respectively. In case of columns, ρ_{tot} and ρ_w were respectively set to 1.70% and 1%. A Normal distribution was assigned to ρ_w with mean of 3.10% and CoV = 0.73% in case of columns and mean of 3.75% and CoV = 0.14% in case of beams (CEN, 2004).

4. FRAGILITY ANALYSIS

The authors carried out fragility analysis by means of a *Mathematica*® script for masonry infill walls, and *Matlab*® combined with *OpenSees*® (McKenna et al. 2004) for frames. A Monte Carlo sampling procedure was used to generate realizations of both demand and capacity accounting for uncertainties in materials, geometry and capacity models. Each building subclass was defined by a set of nominal values for material properties, dimensions of infill

walls and frames, and reinforcement ratios. Landslide velocity was assumed to range between 0 and 30 with step 1. For each capacity model and velocity level, 10^2 samples of demand-related variables and structural parameters were randomly generated from their own statistical distributions to fit and convolve distributions for landslide demand and capacity, and to fit lognormal fragility curves. In case of out-of-plane loaded infills, distributions of p_{eq} and w were determined through Eqs. (1)–(3), allowing fragility curves corresponding to DS1 to be determined. In case of frames, Monte Carlo sampling and nonlinear frame analysis were respectively performed in *Matlab*® and *OpenSees*®. A force-controlled, incremental static analysis of frames was carried out and the maximum rotation demand corresponding to p_{eq} was recorded. That procedure was repeated to the total number of simulations, enabling a set of maximum rotation demands to be determined. The same number of rotation capacity realizations was randomly generated in terms of θ_y and θ_u. Figure 4 and Figure 5 respectively show fragility curves derived for bare and infilled frames of EC8-compliant buildings. The probability of exceeding a damage state is denoted as P_f. The interaction between masonry infills and RC frames drastically changes the landslide fragility, shifting the median to higher velocity levels. In addition, in-plane failure of infill walls is more probable than yielding rotation if $0 \leq v \leq 26$ m/s. This always occurs in case of gravity-load designed buildings (Figure 6 and Figure 7).

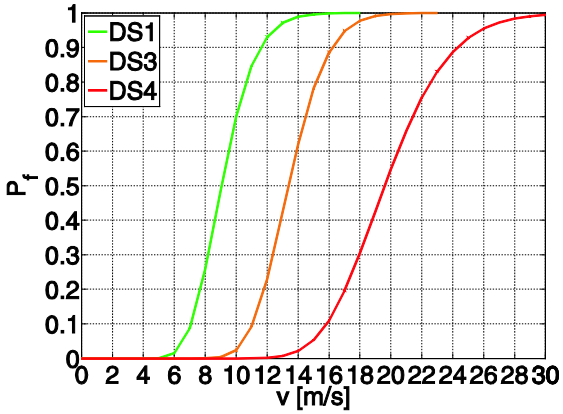

Figure 4: Fragility curves of EC8-compliant bare frames.

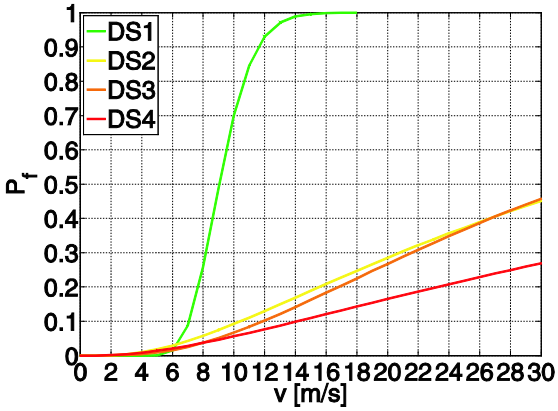

Figure 5: Fragility curves of EC8-compliant infilled frames.

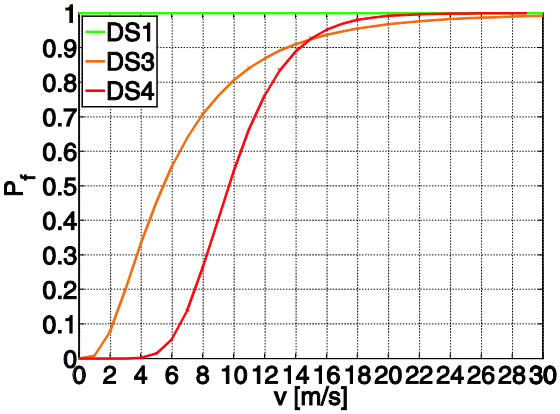

Figure 6: Fragility curves of gravity-load designed bare frames.

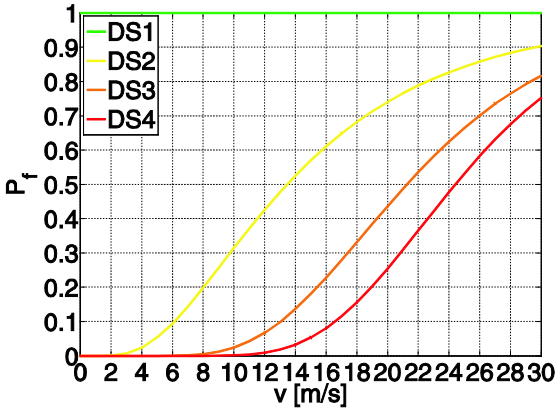

Figure 7: Fragility curves of gravity-load designed infilled frames.

Weak infills did not resist even geostatic pressures resulting in $P_f = 1$ at any velocity level. Fragility curves of gravity-load designed buildings are more distinct each other. The median velocity corresponding to DS2 is notably lower than that

related to EC8-compliant buildings.

5. CONCLUSIONS

Landslide fragility of RC framed buildings has been found to be significantly different for gravity-load designed and earthquake-resistant RC buildings. Masonry infill walls play a key role, inducing major changes in all fragility curves. The methodology and results of this study may be used to assess landslide-related losses at regional scale.

6. REFERENCES

Abrams, D., Angel, R., and Uzarski, J. (1996). "Out-of-plane strength of unreinforced masonry infill panels", *Earthquake Spectra*, 12(4), 825–844.

Bertoldi, S., Decanini, L.D., and Gavarini, G.C. (1993). "Telai tamponati soggetti ad azioni sismiche: Un modello semplificato – Confronto sperimentale e numerico", *Proc., 6th Italian Conf. on Earthquake Engineering*, Perugia, Italy (in Italian).

Biskinis, D.E., Roupakias, G.K., and Fardis, M.N. (2004). "Degradation of shear strength of reinforced concrete members with inelastic cyclic displacements", *ACI Structural Journal*, 101(6), 773–783.

Comité Européen de Normalisation (CEN) (2004). "Eurocode 8: Design of structures for earthquake resistance – Part 1: General rules, seismic actions and rules for buildings", EN 1998-1, Brussels, Belgium.

Comité Européen de Normalisation (CEN) (2005). "Eurocode 8: Design of structures for earthquake resistance – Part 3: Assessment and retrofitting of buildings", EN 1998-3, Brussels, Belgium.

Corominas, J., van Westen, C., Frattini, P., et al. (2013). "Recommendations for the quantitative analysis of landslide risk", *Bulletin of Engineering Geology and the Environment*, 73(2), 209–263.

Fardis, M.N. (2007). *LESSLOSS — Risk mitigation for earthquakes and landslides. Guidelines for displacement-based design of buildings and bridges*, Report No. 5/2007, IUSS Press, Pavia, Italy.

Fotopoulou, S.D., and Pitilakis, K.D. (2013). "Fragility curves for reinforced concrete buildings to seismically triggered slow-moving slides", *Soil Dynamics and Earthquake Engineering*, 48, 143–161.

Galasso, C., Maddaloni, G., and Cosenza, E. (2014) Uncertainly analysis of flexural overstrength for capacity design of RC beams, *ASCE Journal of Structural Engineering*, 140(7), 04014037.

Hak, S., Morandi, P., Magenes, G., and Sullivan, T.J. (2012). "Damage control for clay masonry infills in the design of RC frame structures", *Journal of Earthquake Engineering*, 16(sup1), 1–35.

Italian Ministry of Infrastructures and Transportation (IMIT) (2009). "Circolare n. 617 del 02.02.2009: Istruzioni per l'applicazione delle «Nuove Norme Tecniche per le Costruzioni» di cui al decreto ministeriale 14 gennaio 2008", Rome, Italy (in Italian).

Italian National Research Council (INRC) (2013). "Istruzioni per la valutazione affidabilistica della sicurezza sismica di edifici esistenti", CNR-DT 212, Rome, Italy (in Italian).

Masi, A., and Vona, M. (2012). "Vulnerability assessment of gravity-load designed RC buildings: Evaluation of seismic capacity through non-linear dynamic analyses", *Engineering Structures*, 45, 257–269.

Mavrouli, O., Fotopoulou, S., Pitilakis, K.D., et al. (2014). "Vulnerability assessment for reinforced concrete buildings exposed to landslides", *Bulletin of Engineering Geology and the Environment*, 73(2), 265–289.

McKenna, F., Fenves, G.L., and Scott, M.H. (2004). OpenSees: Open system for earthquake engineering simulation, *Pacific Earthquake Engineering Research Center*, University of California, Berkeley, California, USA.

Parisi, F., and Augenti, N. (2013). "Seismic capacity of irregular unreinforced masonry walls with openings", *Earthquake Engineering and Structural Dynamics*, 42, 101–121.

Petley, D.N. (2012). "Global patterns of loss of life from landslides", *Geology*, 40(10), 927–930.

Porter, K., Kennedy, R., and Bachman, R. (2007). "Creating fragility functions for performance-based earthquake engineering", *Earthquake Spectra*, 23(2), 471–489.

Pregnolato, M., Galasso, C., and Parisi, F. (2015). Existing Flood Vulnerability and Fragility Relationships: Compendium and Guide for selection, *ASCE-ASME Journal of Risk and Uncertainty in Engineering Systems, Part A: Civil Engineering* (to be submitted).

Royal Decree (1939). "Regio-Decreto Legge 16 novembre 1939 n. 2229: Norme per l'esecuzione delle opere in conglomerato cementizio semplice od armato", Rome, Italy (in Italian).

Sapir, D.G., and Misson, C. (1992). "The development of a database on disasters", *Disasters*, 16(1), 74–80.

Sezen, H., and Moehle, J.P. (2004). "Shear strength model for lightly reinforced concrete columns", *ASCE Journal of Structural Engineering*, 130(11), 1692–1703.

Stafford Smith, B. (1966). "Behaviour of square infilled frames", *ASCE Journal of the Structural Division*, 92(1), 381–403.

Verderame, G.M., Manfredi, G., and Frunzio, G. (2001a). "Le proprietà meccaniche dei calcestruzzi impiegati nelle strutture in cemento armato realizzate negli anni '60", *Proc., 10th Italian Conf. on Earthquake Engineering*, Potenza-Matera, Italy (in Italian).

Verderame, G.M., Stella, A., and Cosenza, E. (2001b). "Le proprietà meccaniche degli acciai impiegati nelle strutture in cemento armato realizzate negli anni '60", *Proc., 10th Italian Conf. on Earthquake Engineering*, Potenza-Matera, Italy.

Zhu, L., Elwood, K., and Haukaas, T. (2007). "Classification and seismic safety evaluation of existing reinforced concrete columns", *ASCE Journal of Structural Engineering*, 103(9), 1316–1330.